

Some Comments About The High Energy Limit of QCD

Larry McLerran

Physics Department and Riken Brookhaven Center

PO Box 5000, Brookhaven National Laboratory, Upton, NY 11973 USA

Abstract

I argue that the physics of the scattering of very high energy strongly interacting particles is controlled by a new, universal form of matter, the Color Glass Condensate. This matter is the dominant contribution to the low x part of a hadron wavefunction. In collisions, this matter almost instantaneously turns into a Glasma. The Glasma initially has strong longitudinal color electric and magnetic fields, with topological charge. These fields melt into gluons. Due to instabilities, quantum noise is converted into classical turbulence, which may be responsible for the early thermalization seen in heavy ion collisions at RHIC.

1 The High Energy Limit

The high energy limit of QCD is the limit where the energy of collisions goes to infinity, but the typical momentum transfer is finite. This momentum transfer can be much larger than Λ_{QCD} , but it is to remain fixed. This is not the short distance limit, where both momentum transfer and energy go to infinity. The short distance limit is understood using weak coupling perturbation theory. The high energy limit is that of non-perturbative phenomena such as Pomerons, Reggeons, unitarization etc. etc. One of the purposes of this lecture is to convince the reader that this non-perturbative limit of QCD is also a weak coupling limit

The Bjorken x variable can be understood as the ratio of the energy of the constituent of a hadron to that of the hadron itself in the reference frame where the hadron has large energy. The typical minimal value of x is

$$x_{min} \sim \Lambda_{QCD}/E_{hadron} \quad (1)$$

The minimal value decreases as the hadron energy increases.

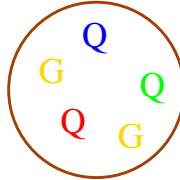
A hadron wavefunction has many different components. This is illustrated in Fig. 1. A nucleon has a Fock space component with three quarks and no gluons, with an extra gluon and with many extra gluons. The components which control low energy scattering are those with three quarks and a few gluons. For high energy scattering processes, the typical matrix elements are those with three quarks, many quark anti-quark pairs, and even more gluons.

2 What is the Color Glass Condensate?

The original ideas for the Color Glass Condensate were motivated by the result for the HERA data on the gluon distribution function shown in Fig. 2(a) [1] The gluon density is rising rapidly as a function of decreasing x . This was expected in a variety of theoretical works[2]-[4] and has the implication that the real physical transverse density of gluons must increase.[2]-[3],[5]. This follows because total cross sections rise slowly at high energies but the number of gluons is rising rapidly. The gluons must fit inside the size of the hadron.

This is shown in Fig. 2(b). This led to the conjecture that the density of gluons should become limited, that is, there is gluon saturation. [2]-[3], [5] Actually, I argue that as one goes to higher energy, a hadron becomes a tightly packed system of gluons larger than some size scale. For smaller gluons there are holes. As one increases the energy, one still adds in more gluons, but these gluons are small enough that they fit into the holes. Because in quantum mechanics, we interpret size as wavelength as inversely proportional to momentum,

In rest frame
Valence quarks
and occasional glue
and sea quarks



In infinite momentum
frame

Wall of lots and
lots of glue at near
light speed



Figure 1: The various components of the hadron wavefunction.

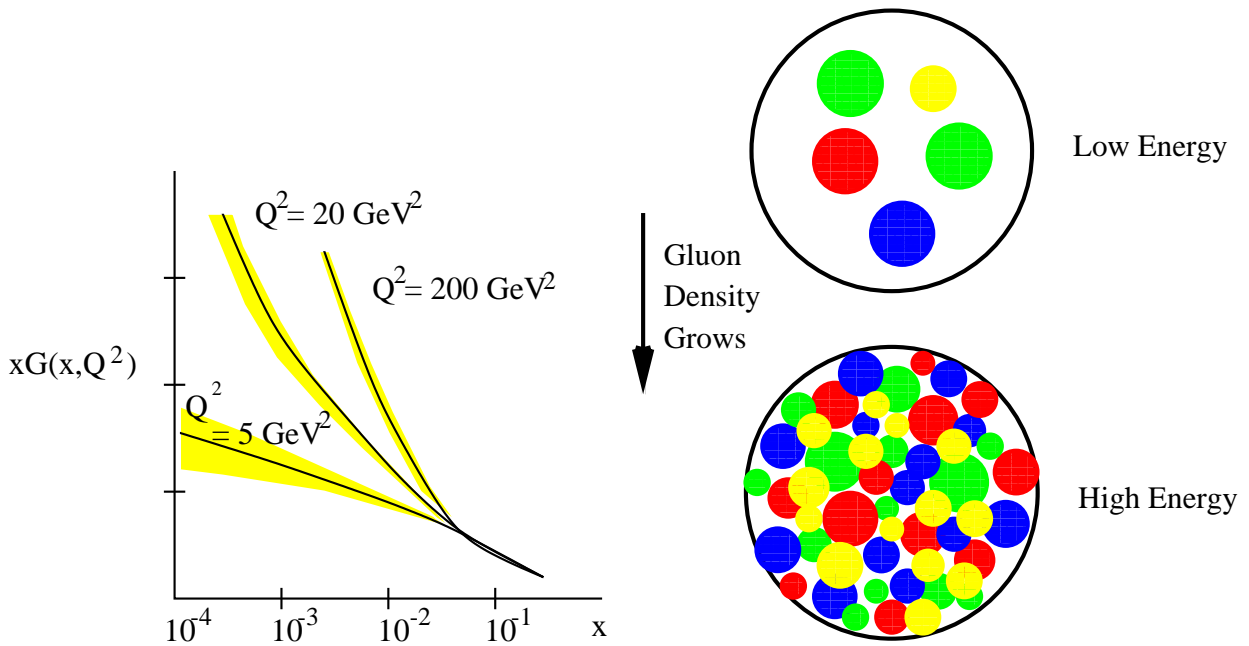


Figure 2: (a) The HERA data for the gluon distribution function as a function of x for various values of Q^2 . (b) A physical picture of the low x gluon density inside a hadron as a function of energy.

at high energies, the gluons are tightly packed for gluons below some momentum, and are filling in above that momentum. There is therefore a critical momentum, the saturation momentum, which characterizes the filling. This saturation momentum increases as the energy increases, so the total number of gluons can increase without bound.

The low x gluons therefore are closely packed together, and become more closely packed as the energy increases. The strong interaction strength must become weak, $\alpha_S \ll 1$. Weakly coupled systems should be possible to understand from first principles in *QCD*. [5]-[6]

This weakly coupled system is called a Color Glass Condensate (CGC) for reasons we now enumerate: [6]

- **Color** The gluons which make up this matter are colored.
- **Glass** The gluons at small x are generated from gluons at larger values of x . In the infinite momentum frame, these larger momentum gluons travel very fast and their natural time scales are Lorentz time dilated. This time dilated scale is transferred to the low x degrees of freedom which therefore evolve very slowly compared to natural time scales. This is the property of a glass.
- **Condensate** The phase space density

$$\rho = \frac{1}{\pi R^2} \frac{dN}{dy d^2 p_T} \quad (2)$$

is generated by a trade off between a negative mass-squared term linear in the density which generates the instability, $-\rho$ and an interaction term $\alpha_S \rho^2$ which stabilizes the system at a phase space density $\rho \sim 1/\alpha_S$. Because $\alpha_S \ll 1$, this means that the quantum mechanical states of the system associated with the condensate are multiply occupied. They are highly coherent, and share some properties of Bose condensates. The gluon occupation factor is very high, of order $1/\alpha_S$, but it is only slowly (logarithmically) increasing when further increasing the energy, or decreasing the transverse momentum. This provides saturation and cures the infrared problem of the traditional BFKL approach. [7]

One can understand the high phase space occupancy $1/\alpha_S$ from simple arguments. The momentum scale in the phase space distribution is the De Broglie wavelength of the gluons which we can interpret as the size of the gluons. The gluons of fixed size will densely occupy the system until there are $1/\alpha_S$ gluons of fixed size closely packing the system. The gluons interact with strength α_S , so that when $1/\alpha_S$ sit on top of one another, they act coherently like a hard sphere with interaction strength of order 1.

Implicit in this definition is a concept of fast gluons which act as sources for the colored fields at small x . These degrees of freedom are treated differently than the fast gluons which are taken to be sources. The slow ones are fields. There is an arbitrary X_0 which separates these degrees of freedom. This arbitrariness is cured by a renormalization group equation which requires that physics be independent of X_0 . In fact this equation determines much of the structure of the resulting theory as its solution flows to a universal fixed point. [6]-[9]

There is evidence which supports this picture. One piece is the observation of limiting fragmentation. This phenomena is that if particles collide at some fixed center of mass energy and the distribution of particles are measured as a function of their longitudinal momentum from the longitudinal momentum of one of the colliding particles, then these distributions do not change as one goes to higher energy, except for the new degrees of freedom that appear. This is true near zero longitudinal momentum in the center of mass frame because new degrees of freedom appear as the center of mass energy is increased. In the analogy with the CGC, the degrees of freedom, save the new ones added in at low longitudinal momentum, are the sources. The fields correspond to the new degrees of freedom. The sources are fixed in accord with limiting fragmentation. One generates an effective theory for the low longitudinal momentum degrees of freedom as fixed sources above some cutoff, and the fields generated by these sources below the cutoff. A recent measurement of limiting fragmentation comes from the Phobos experiment at RHIC shown in Fig. 3 [10]

Of course the perfect scaling of the limiting fragmentation curves is only an approximation. As shown by Jalilian-Marian, the limiting fragmentation curves are given by the total quark, antiquark and gluon distribution functions of the fast particle measured at a momentum scale Q_{sat}^2 appropriate for the particle that it collides with. [11] The saturation momentum Q_{sat} will play a crucial role in our later discussion. It is a momentum scale which is determined by the density of gluons in the CGC

$$\frac{1}{\pi R^2} \frac{dN}{dy} \sim \frac{1}{\alpha_S} Q_{sat}^2 \quad (3)$$

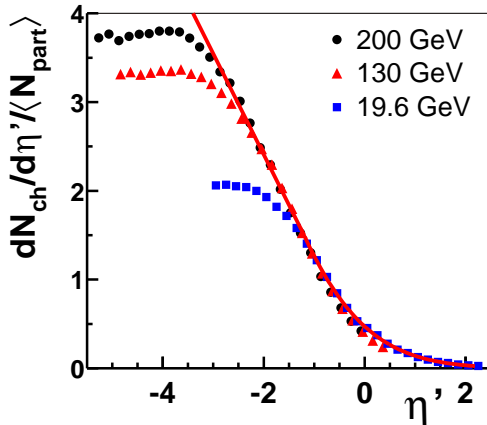


Figure 3: Limiting fragmentation as measured in the Phobos experiment at RHIC.

The saturation momentum turns out to depend on the total beam energy because the longitudinal momentum scale of the target particle at fixed x of the projectile will depend upon the beam energy. It is nevertheless remarkable how small these violations appear to be.

The CGC may be defined mathematically by a path integral:

$$Z = \int_{x_0} [dA][dj] \exp(iS[A, j] - \chi[j]) \quad (4)$$

What this means is that there is an effective theory defined below some cutoff in x at X_0 , and that this effective theory is a gluon field in the presence of an external source j . This source arises from the quarks and gluons with $x \geq X_0$, and is a variable of integration. The fluctuations in j are controlled by the weight function $\chi[j]$. It is $\chi[j]$ which satisfies renormalization group equations which make the theory independent of X_0 . [6],[8]-[9],[12]-[14]. The equation for χ is called the JIMWLK equation. This equation reduces in appropriate limits to the BFKL and DGLAP evolution equations.[4], [15] The theory above is mathematically very similar to that of spin glasses.

There are a variety of kinematic regions where one can find solutions of the renormalization group equations which have different properties. There is a region where the gluon density is very high, and the physics is controlled by the CGC. This is when typical momenta are less than a saturation momenta which depends on x ,

$$Q^2 \leq Q_{sat}^2(x) \quad (5)$$

The dependence of x has been evaluated by several authors, [2],[16]-[18], and in the energy range appropriate for current experiments has been determined by Triantafyllopoulos to be

$$Q_{sat}^2 \sim (x_0/x)^\lambda \text{ GeV}^2 \quad (6)$$

where $\lambda \sim 0.3$. The value of x_0 is not determined from the renormalization group equations and must be found from experiment.

The kinematic region corresponding to the CGC is shown in Fig. 4.

There is also a region of very high Q^2 at fixed x , where the density of gluons is small and perturbative QCD is reliable. It turns out there is a third region intermediate between high density and low where there are universal solutions to the renormalization group equations and scaling in terms of Q_{sat}^2 . [17] In this region and in the region of the CGC, distribution functions are universal functions of only $Q^2/Q_{sat}^2(x)$. The extended scaling region is when

$$Q_{sat}^2 \leq Q^2 \leq Q_{sat}^4/\Lambda_{QCD}^2 \quad (7)$$

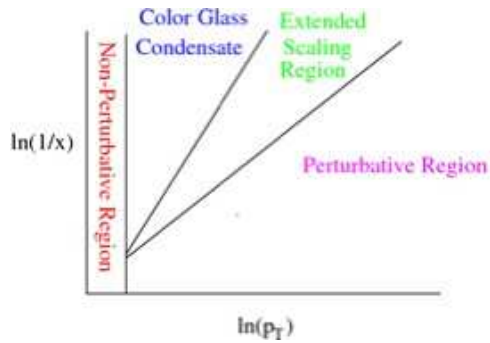


Figure 4: The kinematic regions of the Color Glass Condensate.

3 What is the Form of the Color Glass Fields?

One can simply compute the form of the Color Glass fields. If we work in a frame where the hadron has a large momentum, the $z-t \sim 0$. The only big component of $F^{\mu\nu}$ is F^{i+} where

$$x^\pm = (z \pm t)/\sqrt{2} \quad (8)$$

If we set $F_{i-} = 0$, then simple algebra tells us that the big field strengths are E and B , and that

$$\vec{E} \perp \vec{B} \perp \vec{z} \quad (9)$$

The fields are plane polarized perpendicular to the beam direction. These are the Lienard-Wiechart potentials which correspond to a Lorentz boosted Coulomb field. They exist within the Lorentz contracted sheet and have a longitudinal extent corresponding to the fast moving sources. (The vector potential corresponding to these field is extended, and the wee gluons corresponding to these fields are extended over a larger longitudinal size scale). The fields have random polarizations and colors. This is shown in Fig. 5.

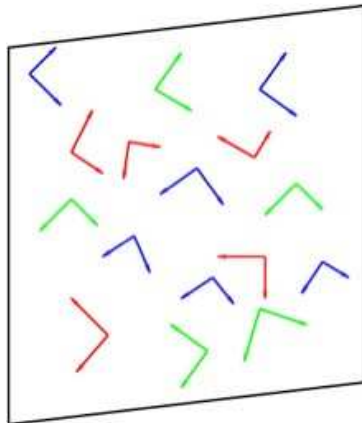


Figure 5: The color glass field.

4 What is the CGC Good For?

The CGC provides a unified description of deep inelastic structure functions, of deep inelastic diffraction and of hadron-hadron collisions at high energies. It is the high energy limit of QCD. As such, it has many tests to pass before being accepted as a correct description. Over the last several years, there have been many qualitative and semi-quantitative successes of

this description. It also provides an intuitively plausible and mathematically consistent description of such phenomena.

One can compute the x dependence of the saturation momentum.[17]-[18] This solutions results from renormalization group equations. The results agree with Hera phenomenology.[19] In particular, within the same description one can compute both deep inelastic structure functions and diffractive structure functions.

In addition, the CGC predicts the existence of geometric scaling.[20] Geometric scaling means that the cross section for deep inelastic scattering of a virtual photon from a hadron depends only upon the scale invariant ratio Q^2/Q_{sat}^2 , and not independently Q^2 and x . Such scaling is shown in Fig. 6 for x values of $x < 10^{-2}$.

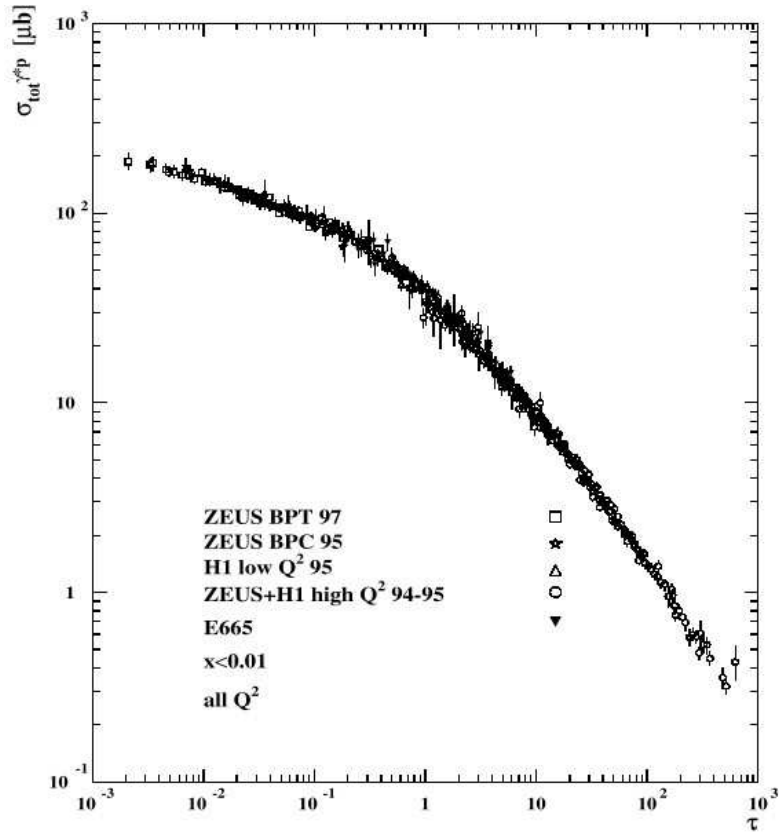


Figure 6: Geometric Scaling as seen at Hera..

The total cross section for hadron-hadron scattering is a slowly varying function of energy as shown in Fig. 7. The Color Glass Condensate provides a heuristic explanation of this.[21]-

The total hadronic cross section:

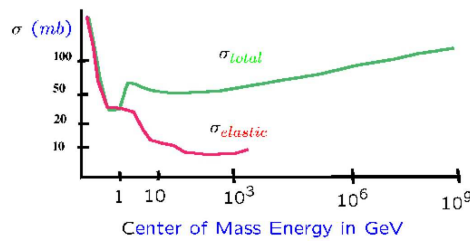


Figure 7: The total hadronic cross section as a function of energy..

[23] We assume the distribution of gluons in the transverse plane of a hadron as a function of energy factorizes,

$$\frac{dN}{d^2r_T dx} \sim (x_0/x)^\lambda e^{-2m_\pi r_T} \quad (10)$$

where the exponential fall off should be of the form shown at large r_T , since the lowest mass particle exchange with isospin zero is two pions. The cross section for a particle of some size to penetrate the hadron, and have a large probability to scatter occurs when this density is some fixed number. Therefore

$$\sigma \sim R^2 \sim \ln^2(1/x) \sim \ln^2(E/E_0) \quad (11)$$

This behaviour is the Froissart bound for cross sections, and describes high energy scattering reasonably well. Its origin is the trade off in rapidly falling impact parameter profile against rapidly rising density of partons.

One of the remarkable predictions of the Color Glass Condensate was the multiplicity of particles produced in heavy ion collisions at RHIC.[24] The multiplicity of saturated gluons inside a nucleus should scale as

$$\frac{dN}{dy} \sim \frac{1}{\alpha_S} \pi R^2 Q_{sat}^2 \quad (12)$$

The energy dependence of Q_{sat} is known, and the dependence on centrality should be proportional to N_{coll} , the number of nucleons colliding, at not too high an energy. Assuming the hadron multiplicity is proportional to the number of produced gluons gives the plot shown in Fig. 8. [25]

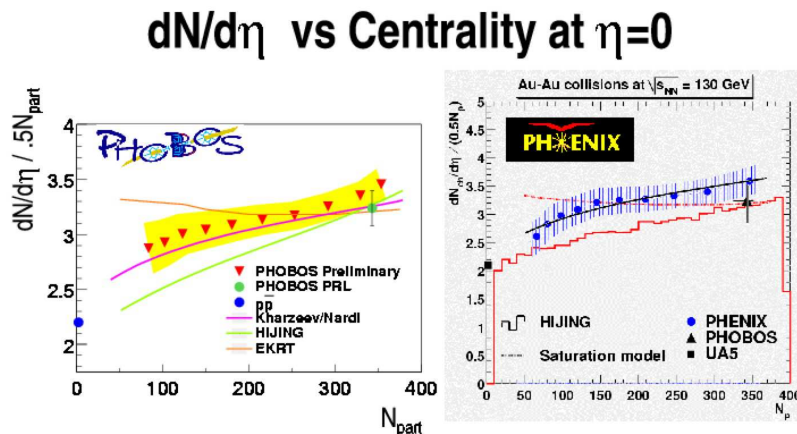


Figure 8: The multiplicity as a function of energy observed at the RHIC

Experiments using deuterons on nuclei in the fragmentation region of the deuteron also test ideas about how the gluon distribution is modified by the Color Glass Condensate. If one uses a multiple collision model to infer the change of the distribution of produced high momentum particles, then there should be more particles at high p_T for intermediate to high p_T . Because of probability conservation, there should be a depletion of low momentum particles. At very high p_T , where multiple scattering should not be important, the distribution should not be changed.

The CGC on the other hand predicts an additional phenomenon. Since there is a high density media, the QCD evolution equations stop running when the scale becomes of the order of the saturation momentum. This means that in nuclei which have a larger saturation momentum than the proton, that there should be a net depletion of particles.

The experimental measurements are in accord with CGC predictions at forward rapidities.[25] The effect is shown as a function of centrality of the collisions in Fig. 9. Forward rapidities

correspond to small x values for the deuteron wavefunction. At larger values of x , the multiple scattering effects dominate, and there is an enhancement as a function of centrality. For the central region of gold-gold collisions at RHIC energies, the effects almost cancel one another.

In the future years, there will be increasingly stringent tests arising at RHIC, LHC and potentially eRHIC. Theoretically, we are just beginning to understand the properties of this matter. New ideas concerning the structure of the underlying theory and the breadth of phenomena it describes are changing the way we think about high energy density matter.

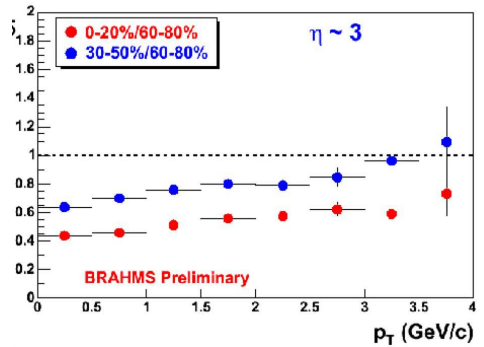


Figure 9: The ratio of single particle production in central to peripheral collisions at forward rapidity as a function of centrality as measured in the Brahm's experiment.

5 What is the Glasma?

When two sheets of colored glass collide, the properties of the matter are changed in the time it takes light to propagate across the sheets of colored glass. [26]-[30] In Fig. 10 a, the sheets of colored glass approach one another. The colored fields in the two sheets form a condensate

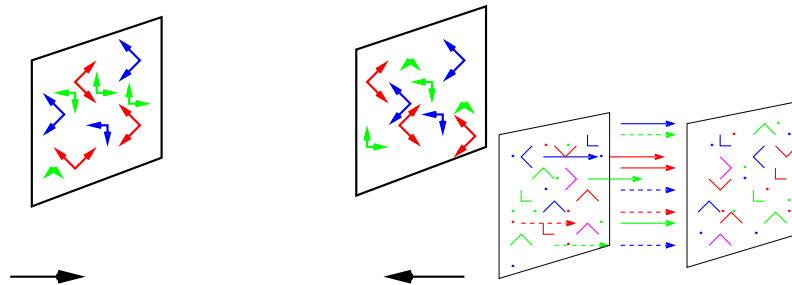


Figure 10: (a) Two sheets of colored glass approach one another. (b) After the collisions, Glasma is formed in the region between the sheets.

of Weizsacker-Williams fields disordered in polarization and color. In the time it takes the sheets to pass through one another, the fast degrees of freedom gain a density of color electric and magnetic charge. The density of charge on each sheet is equal and opposite. This is a consequence of the classical fields which are generated by the source sheets of color glass. Attached to the region away from the collision region is a pure two dimensional transverse vector potential. This potential has no color electric and magnetic field until the nuclei pass through one another, since then the vector potential of one sheet multiplies the field of the other. Then sources are set up according to the Yang-Mill equations

$$\begin{aligned}\rho_E^a &= f^{abc} A^b \cdot E^c \\ \rho_B^a &= f^{abc} A^b \cdot B^c\end{aligned}\tag{13}$$

These colored electric and magnetic charges generate longitudinal color electric and magnetic fields as shown in Fig. 10b. The reason why both electric and magnetic fields are made is because of the duality of the Yang-Mill equations under $E \leftrightarrow B$, and because the initial fields of the colored glass have this symmetry.

When there is a nonzero $E \cdot B$ means that there is a topological charge induced. This Chern Simons charge is

$$\partial \cdot K = \alpha_S \kappa E \cdot B \quad (14)$$

where κ is a constant. This topological charge generates helicity non-conservation. To understand how this works, consider a parallel electric and magnetic field in electrodynamics. An electron is accelerated and rotates around a magnetic field in the opposite sense to a positron. Therefore both the electron and positron acquire the same vorticity. The sign of the vorticity depends upon the sign of $E \cdot B$. For an extended charge distribution, corresponding to a hadron, we expect that there will be a similar biasing of the helicity distributions of hadrons.

The classical equations after the collision evolve in time and become dilute as a consequence of the non-linearities of the Yang-Mills equation. There is a simple solution to this problem which has an invariance under Lorentz boosts along the collision axis. It has however been recently show that this solution is unstable with respect to small non boost invariant solutions. These solutions grow in magnitude as time evolves, amplifying small initial fluctuations into full scale chaotically turbulent solutions. This turbulence and its rapid onset may be responsible for the early thermalization seen at RHIC.

One of the outstanding problems of the Glasma is to understand how these initial fluctuations are formed. They presumably arise from the initial wavefunction of the nuclei. Then the classical instabilities of the Yang-Mills equations amplify these fluctuations, and if one waits long enough, the fluctuations dominate the classical solution. Therefore, quantum noise is amplified to such an effect that it becomes as large as the classical fields. Whether or not there is sufficient time in RHIC or LHC energy collisions for these effects to become significant is not yet known.

6 The Emerging Picture of RHIC Collisions

The emerging picture we have of RHIC collisions is shown in Fig. 11 In the initial state,

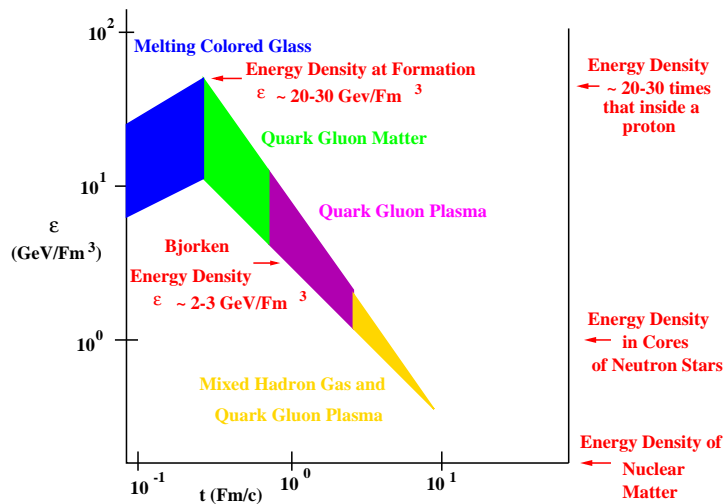


Figure 11: The Emerging Picture of RHIC collisions

there are two sheets of colored glass. They collide and produce a glasma, which melts into gluons. During the melting, or perhaps afterwards, the quarks and gluons thermalize. This eventually makes a Quark Gluon Plasma. Data from RHIC indicates this happens very rapidly, on a time scale of the order of 1 Fm/c . In Fig. 11, I have presented the

typical energy scales and times involved. The scale of energy comes from the measurements of multiplicities and HBT radii at RHIC. The range in estimates comes from making the radical assumptions of complete thermalization and no thermalization of the gluons. The bottom line is that the scales are large and the times probed are very early.

7 Summary

In addition to the Quark Gluon Plasma, other interesting new forms of matter are being probed at RHIC. These are the Color Glass Condensate and the Glasma. These forms of matter allow us to test ideas about QCD when the non-linearities of QCD are present, yet to use weak coupling methods. At the LHC, the potential for studying such new form of matter is great due to the larger range in x and typical momentum scales.

8 Acknowledgements

I gratefully acknowledge conversations with Francois Gelis, Edmond Iancu, Dima Kharzeev, and Tuomas Lappi Genya Levin, and Raju Venugopalan on the subject of this talk. I thank Michael Praszalowicz and Andrzej Bialas for their kind hospitality at Zakopane.

This manuscript has been authorized under Contract No. DE-AC02-98CH0886 with the U. S. Department of Energy.

References

- [1] J. Breitweg et. al. *Eur. Phys. J.* **67**, 609 (1999).
- [2] L. V. Gribov, E. M. Levin and M. G. Ryskin, *Phys. Rept.* **100**, 1 (1983).
- [3] A. H. Mueller and Jian-wei Qiu, *Nucl. Phys.* **B268**, 427 (1986); J.-P. Blaizot and A. H. Mueller, *Nucl. Phys.* **B289**, 847 (1987).
- [4] L.N. Lipatov, *Sov. J. Nucl. Phys.* **23** (1976), 338;
E.A. Kuraev, L.N. Lipatov and V.S. Fadin, *Sov. Phys. JETP* **45** (1977), 199;
Ya.Ya. Balitsky and L.N. Lipatov, *Sov. J. Nucl. Phys.* **28** (1978), 822.
- [5] L. D. McLerran and R. Venugopalan, *Phys. Rev.* **D49**, 2233(1994); 3352 (1994); **D50**, 2225 (1994).
- [6] E. Iancu, A. Leonidov and L. D. McLerran, *Nucl. Phys.* **A692**, 583 (2001); E. Ferreiro E. Iancu, A. Leonidov and L. D. McLerran, *Nucl. Phys.* **A710**,373 (2002).
- [7] E. Iancu and L. McLerran, *Phys. Lett.* **B510**, 145 (2001).
- [8] J. Jalilian-Marian, A. Kovner, L. McLerran and H. Weigert, *Phys. Rev.* **D55** (1997), 5414.
- [9] J. Jalilian-Marian, A. Kovner, A. Leonidov and H. Weigert, *Nucl. Phys.* **B504** (1997), 415; *Phys. Rev.* **D59** (1999), 014014.
- [10] B. Back et. al. *Phys. Rev. Lett.* **91**, 052303 (2003).
- [11] J. Jalilian-Marian, *Phys. Rev.*, **C70** 027902 (2004)
- [12] I. Balitsky, *Nucl. Phys.* **B463** (1996), 99.
- [13] Yu. V. Kovchegov, *Phys. Rev.* **D60** (1999), 034008; *ibid.* **D61** (2000), 074018.
- [14] A. H. Mueller, *Phys.Lett.* **B523**, 243 (2001)
- [15] V.N. Gribov and L.N. Lipatov, *Sov. Journ. Nucl. Phys.* **15** (1972), 438; G. Altarelli and G. Parisi, *Nucl. Phys.* **B126** (1977), 298; Yu. L. Dokshitzer, *Sov. Phys. JETP* **46** (1977), 641.
- [16] E. Levin and K. Tuchin, *Nucl. Phys.* **A691**, 779 (2001)
- [17] E. Iancu, K. Itakura and L. McLerran, *Nucl. Phys.* **A708**, 327 (2002).
- [18] A. H. Mueller and V. N. Triantafyllopoulos, *Nucl.Phys.* **B640**, 331 (2002). D. N. Triantafyllopoulos, *Nucl. Phys.* **B648**, 293 (2003).

- [19] K. Golec-Biernat and M. Wustoff, *Phys. Rev.* **D60** 114023 (1999).
- [20] K. Golec Biernat, Anna Statso, and J. Kwiecinski, *Phys. Rev. Lett.* **86** 596 (2001).
- [21] A. Kovner and U. Wiedemann, *Phys. Lett.* **B551** 311 (2003);
- [22] E. Ferreiro, E. Iancu, K. Itakura and L. McLerran, *Nucl. Phys.* **A710** 373 (2002)
- [23] L. McLerran and T. Ikeda, *Nucl. Phys.* **A756** 385 (2005).
- [24] D. Kharzeev and M. Nardi, *Phys. Lett.* **B507** 121 (2001).
- [25] Reports of the Star, Phenix, Phobos and Brahms experimental collaborations in *Nucl. Phys* **A757** (2005) Brahms Collaboration p 1; Phobos Collaboration p 28; Star Collaboration p 102; Phenix Collaboration 184.
- [26] A. Kovner, L. McLerran and H. Weigert, *Phys. Rev.* **D52** 3809 (1995); 6231 (1995).
- [27] A. Krasnitz and R. Venugopalan, *Nucl. Phys.* **B557** 237 (1999); *Phys. Rev. Lett.* **84** 4309 (2000); *Phys. Rev. Lett.* **86** 1717 (2001).
- [28] A. Krasnitz, Y. Nara and R. Venugopalan, *Phys. Rev. Lett.* **87** 192302 (2001); *Nucl. Phys.* **A717** 268 (2003)
- [29] T. Lappi, *Phys. Rev.* **C67** 054903 (2003).
- [30] T. Lappi and L. McLerran, *Nucl. Phys.* **A772** 200 (2006).
- [31] S. Mroczynski, *Phys. Lett.* **B214** 587 (1988); **B314** 118 (1993); **B363**, 26 (1997).
- [32] P. Arnold, J. Lenaghan, and G. Moore, *JHEP* **0308** 002 (2003); P. Arnold, J. Lenaghan, G. Moore and L. Yaffe, *Phys. Rev. Lett.* **94** 072302 (2005)
- [33] P. Romatschke and M. Strikland, *Phys. Rev.* **D68** 036004 (2003); **D70** 116006 (2004).
- [34] P. Romatshke and R. Venugopalan, *Phys. Rev. Lett.* **96** 062302 (2006) .
- [35] A. Dumitru and Y. Nara, *JHEP* **0509** 041 (2005); A. Dumitru, Y. Nara and M. Strikland, *Phys. Lett.* **B621** 89 (2005).